Micellization of Polystyrene–Poly(ethylene oxide) Block Copolymers in Water. 5. A Test of the Star and Mean-Field Models[1]

Renliang Xu[2] and Mitchell A. Winnik*

Department of Chemistry and Erindale College, University of Toronto, Toronto, Ontario, Canada M5S 1A1

Gérard Riess

Ecole Nationale Supérieure de Chimie, 3 rue Werner, 68093 Mulhouse Cedex, France

Benjamin Chu

Department of Chemistry, State University of New York at Stony Brook, Stony Brook, Long Island, New York 11794-3400

Melvin D. Croucher

Xerox Research Centre of Canada, 2660 Speakman Drive, Mississauga, Ontario, Canada L5K 2L1

Received April 16, 1991; Revised Manuscript Received July 29, 1991

ABSTRACT: PS–PEO di- or triblock copolymer micelles of various compositions and molecular weights in water were investigated by light scattering. Characteristic micelle sizes (hydrodynamic radius R_h) were resolved from a secondary association by a combination of static and quasi-elastic light scattering signals. The R_h values for the micelles are in good accord with the scaling relationship of Halperin's star model. The star model then was incorporated into our data analysis to obtain aggregation number N and core radii R_c. With these parameters we are able to test the validity of the Noolandi–Hong mean density micelle model by using their equations to calculate the Flory–Huggins χ parameters for the interaction of PEO–water and PEO–PS. The χ values we obtained are in very good agreement with values in the literature. We found a monotonic dependence of $\chi_{PEO-water}$ on PEO concentration. We note not only that these χ parameters are very difficult to determine by other methods but also that two theoretical models with very different sets of assumptions receive quantitative support from our measurement.

Introduction

When an A–B diblock copolymer or an A–B–A triblock copolymer is placed in a good solvent for the A block but a nonsolvent for the B block, the molecules associate to form micelles.[3-5] These micelles are normally spherical in shape, with a core rich in B chains surrounded by a corona of A chains swollen by the solvent. There have been tremendous advances over the past decade in the theory of block copolymer micelle formation.[6-13] These theories take various forms, but all address common features of the micellization process. In those instances where theory and experiment have been compared, general agreement has been found. There has not been, however, a sufficient number of experiments covering a broad enough range of samples for the more quantitative predictions of these models to be tested.

One source of the paucity of appropriate experiments is the influence of technical details which prevent the assumptions in the theoretical model from being entirely satisfied in the experiments. The theory, for example, considers polymer chains of unique length. It presumes the micelle core to be dense-packed and fluid. The latter assumption is made primarily to ensure that the micelles come to equilibrium under the sample preparation conditions. These assumptions seem to exclude from consideration any micelle in which the insoluble block is composed of a high-T_g polymer such as polystyrene or one such as poly(ethylene oxide) which crystallizes in the core. These particular difficulties can be overcome by the use of solvents or cosolvents which plasticize the core polymer or disrupt its crystallinity. If one tried to take account of these features, it would complicate the theory. Nevertheless, these additives might simplify the behavior of the system and yet be such a small perturbation from the point of view of theory that the parameters of interest, the mean aggregation number N, the core radius R_c, and the corona thickness L, could be compared meaningfully between theory and experiment.

A nice example of this situation was reported by Gast and co-workers[14] with respect to micelle formation by PS–PEO diblock copolymers in cyclopentane. If the solvent was carefully dried, large aggregates with a crystalline PEO interior formed. When traces of moisture were present in the solvent, micelle formation was much more in accord with the predictions of the theories. This can be attributed to localization of the water in the PEO core, disrupting the crystallinity of the PEO phase and bringing the properties of the micelle closer to those assumed in the theoretical models.

We[15] experienced a second type of technical difficulty in the experiments described here. We examined a broad spectrum of poly(ethylene oxide)–polystyrene (PEO–PS) diblock and PEO–PS–PEO triblock copolymers in water. These are samples in which the PS chain lengths are sufficiently short that the T_g of polystyrene does not prevent our samples from coming to equilibrium under various sample preparation conditions.[16] For PS in water, the assumption of a dense-packed core is certainly valid.

* To whom all correspondence should be addressed.

0024-9297/92/2225-0644$03.00/0

Under such circumstances it should be a straightforward matter to determine N values by static light scattering (SLS) measurements of M_w of the micelles and to determine the hydrodynamic radii R_h of the micelles by quasi-elastic light scattering (QELS). Unfortunately, these micelles in water undergo a small extent of secondary association[15,17] to form clusters whose contributions are weighted into the M_w and R_h values obtained from light scattering. One major aspect of this paper is to show how these contributions can be separated and meaningful data obtained.

A second aspect of this paper is to examine our data in light of two quite different types of models of micelle structure. The star model[13] has its origin in the theoretical description of star polymers and develops scaling arguments about the dependence of N, R_c, and L upon the lengths N_A and N_B of the A and B chains, respectively. This model is most appropriate for micelles consisting of a small core from which long A chains protrude to form a large corona.

Mean density models,[8-11] on the other hand, are most appropriate for micelles consisting of a large core and a relatively thin corona. These models ignore correlation effects; but by virtue of the mean-field approximation, they are able to describe many more detailed properties of the micelles. For example, if the appropriate Flory–Huggins χ parameters are available for the A/B, A/solvent, and B/solvent interactions, one can use these theories in conjunction with N_A and N_B values to predict specific values of N, R_c, and L for the micelles formed. One particular shortcoming of these models is that they treat the corona as though there were a uniform segment density of A chains. There are not sufficient experimental data to know if this deficiency is significant from a quantitative point of view.

We emphasize that these two models are not necessarily mutually incompatible. They are derived from two different limiting situations, but scaling relationships based on the mean-field model differ in only very subtle ways from those based on the star model. Unless one had a very large span of block copolymer chain lengths, these differences might be very difficult to observe experimentally.

Our polymers have chain lengths that fall in between the extreme situations to which these two types of models are most appropriate. We have examined a large number of polymers and found that those too rich in PS, where a large core would be anticipated, did not form micelles in water. For those that do form micelles, we use a Laplace inversion technique to obtain values of R_h. These values follow the scaling relationship predicted by the star model. This permits us to then assume the validity of the star model as part of our analysis to get N, R_c, and L values. Our most remarkable finding is that the N, R_c, and L values we obtained in this way are in excellent accord with the predictions of the Noolandi and Hong[8] mean-field model. When these parameters are introduced into the equations developed by Noolandi and Hong, we calculate very reasonable values for χ_{PEO-PS} and for $\chi_{PEO-water}$. We note not only that these χ parameters are very difficult to determine by other methods but also that two theoretical models with very different sets of assumptions receive quantitative support from our measurements.

Theoretical Approach

1. Micelle Models. Current theories picture a block copolymer micelle in terms of a spherical core consisting solely of blocks of polymer B, surrounded by a corona of A chains swollen by the solvent. These micelles are in equilibrium with a small concentration of free polymer molecules ("unimers"), whose concentration is close to the critical concentration (cmc) for micelle formation. To calculate detailed micelle properties, such as the cmc, and the unimer concentration, as well as the aggregation number N and the characteristic radii R_c and R ($=R_c + L$), one needs to describe the total free energy of a micelle solution. The total energy includes the free energy per unit volume of the individual micelles $\Delta g_{micelle}$ plus the mixing free energies of the micelles and of the free polymer molecules.

For most block copolymer micelles, there exists a substantial concentration region $C >$ cmc where micelle–micelle interaction is unimportant. Here the micelle properties are determined by the free energy per unit volume of a single micelle relative to the corresponding free energy of the homogeneous random state. This free energy can be approximated as the sum of three contributions due to the core, the corona, and the interface between them.

$$\Delta g_{micelle} = \Delta g_{core} + \Delta g_{interface} + \Delta g_{corona} \quad (1)$$

The term Δg_{core} accounts for the change in conformational entropy of the B chains upon aggregation, since, in the uniform stretching approximation, the end-to-end distance of the B chains becomes equal to R_c. Δg_{corona} accounts for conformational changes in the A chains. When the distance between graft sites is smaller than the radius of gyration of the free A chains, confinement leads to stretching in the radial direction. Within this framework, the driving force for micelle formation is the lowering of the interface free energy that accompanies association of the B blocks.

One can imagine two limiting situations. In the large-core limit, i.e., $N_B \gg N_A$, the shell thickness is much smaller than the radius of the core. Mean density models treat the volume fraction ϕ_A of A segments in the corona as independent of the distance from the core. With the aid of the mean-field approximation, a description of the total free energy of the micelle solution is possible, and one can calculate specific micelle parameters. With this type of model, one predicts that N is proportional to N_B and that R_c and R increase in proportion to $N_B^{2/3}$.[6-11]

In the opposite limit, i.e., $N_A \gg N_B$, the shell thickness is much larger than the core radius. Due to the larger volume available to the A chains, ϕ_A is no longer a constant but decreases with increasing distance from the core. In the limiting situation where R_c is negligible compared to R, the micelle resembles a star polymer in solution;[18] i.e., A segments form blobs, and the blob size and density depend on its location.[12,13] Under these circumstances, the characteristic radius R is given by the expression

$$R \propto N^{1/5} N_A^{4/5} a \quad (2)$$

with a being the monomer dimension.

Halperin's star model[13] also assumes a self-similar concentration profile for ϕ_A. Thus, the blob size (ξ) increases in proportion to r (the distance from the center). In a spherical shell of radius r and thickness $\xi(r)$ there are N blobs. In a star polymer, N is determined by synthesis, whereas in a micelle, N is self-adjusting. The star model obtains N by minimizing the free energy of single micelles. In this way one obtains very useful scaling relationships between the parameters of interest and the chain lengths of the A and B components:

aggregation number	$N \propto N_B^{4/5}$	(3)
core radius	$R_c \propto N_B^{3/5}$	(4)
micelle radius	$R \propto N_B^{4/25} N_A^{3/5}$	(5)

To accommodate triblock copolymer into these relationships, we consider that each triblock copolymer is equivalent to two A–B diblock copolymers of half the size; i.e., $N_B' = N_B/2$ and $N_A' = N_A/2$, where the primed values are the values used in fitting the polymer to the star model. The aggregation number used in fitting the star model thus is twice the true aggregation number $N' = 2N$. If we want to write an analogous series of expressions, eqs 3–5 have to be "scaled" for triblock copolymers:

aggregation number	$N \propto 2^{-9/5} N_B^{4/5}$	(6)
core radius	$R_c \propto 2^{-3/5} N_B^{3/5}$	(7)
micelle radius	$R \propto 2^{-19/25} N_B^{4/25} N_A^{3/5}$	(8)

2. Flory–Huggins χ Parameters. Because the mean density model has two homogeneous zones, the core and the corona, detailed analytical expressions can be developed to describe the relationship between the free energy of micelles and their constituents. This analysis begins with a much closer examination of the terms contributing to the micelle free energy. Noolandi and Hong considered a micelle made up of a concentrated core and a swollen corona separated by a narrow interphase region of finite width.[8] They divide the free energy difference per unit volume between the random state and the micelle into a sum of five separate contributions.

$$\Delta g = \Delta g_{int} + \Delta g_s + \Delta g_J + \Delta g_{el} + \Delta g_I \quad (9)$$

The first term, Δg_{int}, describes the interaction free energy changes accompanying micelle formation in the pairwise interactions involving the A block, the B block, and the solvent. As seen in Table I,[19] where detailed expressions for these five terms are presented, the interaction free energies are expressed exclusively in terms of the corresponding χ parameters, and the interfacial tension contribution is described separately by the term Δg_I. The term Δg_s includes changes in the combinatorial entropy of solvent molecules in the micelles compared to that in the homogeneous state. In eq 9, the elastic deformations of both the A and B chains are described by Δg_{el}, and Δg_J arises from localization of the joints.

For a given copolymer sample in a given solvent, Δg is a function of R_c, R, N, the micelle concentration C, and three χ parameters. These terms, χ_{AB}, χ_{AS}, and χ_{BS} are the Flory–Huggins interaction parameters between block A, block B, and solvent S, respectively. Micellar dimensions are obtained from minimizing eq 9 with respect to R and R_c. The resulting function must be evaluated numerically.

The intended application of this model is to use known values of the χ parameters in conjunction with N_A and N_B values to predict micelle size. Normally, however, the χ parameters are difficult to obtain, and we explore the possibility that the measured values of N, R_c, and R can be introduced into the model to obtain the desired χ values. If one assumes the core is solvent free, χ_{AB} and χ_{AS} can be obtained from the expressions

$$\chi_{AS}\frac{\partial \Delta g'_{int}}{\partial (R-R_c)} + \frac{\partial \Delta g_s}{\partial (R-R_c)} + \frac{\partial g_J}{\partial (R-R_c)} + \chi_{AB}^{1/2}\frac{\partial \Delta g'_I}{\partial (R-R_c)} + \frac{\partial g_{el}}{\partial (R-R_c)} = 0 \quad (10)$$

$$\chi_{AS}\frac{\partial \Delta g'_{int}}{\partial R_c} + \frac{\partial \Delta g_s}{\partial R_c} + \frac{\partial g_J}{\partial R_c} + \chi_{AB}^{1/2}\frac{\partial \Delta g'_I}{\partial R_c} + \frac{\partial g_{el}}{\partial R_c} = 0 \quad (11)$$

where all the derivatives, listed in Table II, are functions only of R, R_c, and N for a given copolymer sample.

In the present study, we postulate that the equivalent hydrodynamic radius R_h, calculated using the Stokes–Einstein relation, from the translational diffusion coefficient D_T measured by QELS, is effectively the exterior shell boundary of the micelle; i.e., $R_h \approx R$.

3. Static (SLS) and Quasi-Elastic (QELS) Light Scattering. Static and quasi-elastic light scattering techniques were used to measure micelle weights and equivalent hydrodynamic radii of micelles of different block copolymers in aqueous solution.[15] For block copolymers with blocks having different refractive indices, the formulation for static light scattering measurement in dilute micelle solution with a possible second component is[20]

$$\frac{R_{vv}^0}{H'C} = M_{w,app}\left(\frac{\partial n}{\partial C}\right)_A\left(\frac{\partial n}{\partial C}\right)_B + \left(\left(\frac{\partial n}{\partial C}\right)_A^2 - \left(\frac{\partial n}{\partial C}\right)_A\left(\frac{\partial n}{\partial C}\right)_B\right)W_A M_w^A + \left(\left(\frac{\partial n}{\partial C}\right)_B^2 - \left(\frac{\partial n}{\partial C}\right)_A\left(\frac{\partial n}{\partial C}\right)_B\right)W_B M_w^B \quad (12)$$

with H' $(=(4\pi^2 n^2)/(N_A \lambda_0^4))$, with N_A Avogadro's number, n the refractive index of pure solvent, λ_0 the wavelength of light in vacuo, respectively), a constant, R_{vv}^0 the doubly extrapolated (concentration → 0 and scattering angle → 0) excess Rayleigh ratio of the vertically polarized incident beam scattered in a vertically polarized direction, C the block copolymer concentration, $M_{w,app}$ the apparent particle weight, $(\partial n/\partial C)_A$ and $(\partial n/\partial C)_B$ the refractive index increments of components A and B, respectively, W_A and W_B the weight fractions of components A and B, respectively, and M_w^A and M_w^B the molecular weights of components A and B, respectively.

The general formula for the photoelectron-count time-correlation function in the self-beating mode has the form

$$G^{(2)}(\tau) = A(1 + \beta|\int_{\Gamma_{min}}^{\Gamma_{max}} G(\Gamma)\exp(-\Gamma\tau)\,d\Gamma|^2) \quad (13)$$

$G^{(2)}(\tau)$ is the intensity–intensity autocorrelation function at a correlation time τ with β a spatial coherent coefficient for instrument beating efficiency, A a base line, $G(\Gamma)$ the characteristic line-width distribution function, and Γ the characteristic line width with its average value $\bar{\Gamma} = \int \Gamma G(\Gamma)\,d\Gamma$. In our experiments, the ill-posed Laplace inversion of eq 13, from which $G(\Gamma)$ was obtained, was processed by a nonnegatively least-squares (NNLS) algorithm provided by Brookhaven Instrument, Inc. For spherical particles, Γ is related to the translational diffusion coefficient D_T $(=\Gamma/K^2$, with K being the scattering vector) provided that all internal motions are negligible. The extrapolated value of D_T at infinite dilution, D_0, is related to the hydrodynamic radius R_h of the particle by the Stokes–Einstein relation in the hard-sphere limit

$$R_h = k_B T/6\pi\eta D_0 \quad (14)$$

where k_B, T, and η are Boltzmann constant, the absolute

Table I
Equations and Definitions in Free Energy Change of Micelle Systems

symbol	meaning	expression
Δg_{int}	interaction energy	$-\chi_{AB}f_Af_B\phi_C^2 + \chi_{AS}f_A\phi_C\phi_S F_2/G_2 - \chi_{AS}f_A\phi_C\phi_S - \chi_{BS}f_B\phi_C\phi_S$
Δg_S	combinatorial entropy of solvent	$\phi_S\{F_2 \ln (F_2/G_2) + F_3 \ln (F_3/G_3)\}$
Δg_J	energy for localization of joints	$-(\phi_C/(r_A + r_B)) \ln (3R_c^2 b[(\phi_A + \phi_B)/(3\chi_{AB}\phi_A\phi_B)]^{1/2}/R_v^3)$
Δg_{el}	elastic energy	$0.5(\phi_C/(r_A + r_B))(\alpha_A^2 + \alpha_B^2 + 2/\alpha_A + 2/\alpha_B - 6)$
Δg_I	interfacial tension	$[(1/12)(\phi_A + \phi_B)\chi_{AB}\phi_A\phi_B]^{1/2}(3bR_c^2/R_v^3)$
r_i	reduced molecular volume of i (A or B)	$N_i\rho_{oS}/\rho_{oi}$
ρ_{oi}	molar density of component i (mol/mL)	$\rho_{oA} = 0.0257$; $\rho_{oB} = 0.0103$; $\rho_{oS} = 0.0554$
ϕ_C	overall volume fraction of copolymer	$1 - \phi_S$
α_A		$(3/N_A)^{1/2}((R - R_c)/b_A)$ (b_A = Kuhn length of block A = 6.8 Å)
α_B		$(3/N_B)^{1/2}(R_c/b_B)$ (b_B = Kuhn length of block B = 7.1 Å)
G_1	volume fraction of core	$(R_c/R_v)^3$
G_2	volume fraction of shell	$(R/R_v)^3 - (R_c/R_v)^3$
G_3	volume fraction of "free space"	$1 - (R/R_v)^3$
F_2	fraction of solvent in shell	$G_2/\phi_S(1 - f_A\phi_C/G_2)$
F_3	fraction of solvent in "free space"	G_3/ϕ_S
ϕ_A	volume fraction of A in shell	$f_A\phi_C/G_2$
ϕ_B	volume fraction of B in core	$f_B\phi_C/G_1$
R_v	radius of "unit cell"	$(3N(r_A + r_B)/(4\pi N_A\rho_{oS}\phi_C))^{1/3}$
R, R_c	micelle radius and micelle core radius	
f_i	$r_i/(r_A + r_B)$	$b = (b_A + b_B)/2$

Table II
Derivatives of Free Energy Terms in Computation of χ Parameters

$$\frac{\partial \Delta g'_{int}}{\partial (R - R_c)} = \frac{3}{R_v^3}\left(\frac{f_A\phi_C R}{G_2}\right)^2 \qquad \frac{\partial \Delta g'_{int}}{\partial R_c} = \frac{3}{R_v^3}\left(\frac{f_A\phi_C}{G_2}\right)^2 (R^2 - R_c^2)$$

$$\frac{\partial \Delta g_S}{\partial (R - R_c)} = \frac{3R^2}{R_v^3}\left[\ln\left(\frac{F_2}{G_2}\right) - \ln\left(\frac{F_3}{G_3}\right) + \frac{f_A\phi_C}{G_2}\right] \qquad \frac{\partial \Delta g_S}{\partial R_c} = \frac{3}{R_v^3}\left[(R^2 - R_c^2)\ln\left(\frac{F_2}{G_2}\right) - R^2 \ln\left(\frac{F_3}{G_3}\right) + (R^2 - R_c^2)\frac{f_A\phi_C}{G_2}\right]$$

$$\frac{\partial \Delta g_J}{\partial (R - R_c)} = \frac{-3R^2\phi_A\phi_B}{2(r_A + r_B)R_v^3 f_A(\phi_A + \phi_B)} \qquad \frac{\partial \Delta g_J}{\partial R_c} = \frac{-3\phi_A\phi_B}{2(r_A + r_B)R_v^3(\phi_A + \phi_B)}\left(\frac{R^2 - R_c^2}{f_A} + \frac{R_c^2}{f_B}\right)$$

$$\frac{\partial \Delta g'_I}{\partial (R - R_c)} = \frac{-9bR^2R_c^2(2\phi_A\phi_B + \phi_B^2)}{4R_v^6\sqrt{3(\phi_A + \phi_B)\phi_A\phi_B}}\left(\frac{f_A\phi_C}{G_2^2}\right)$$

$$\frac{\partial \Delta g'_I}{\partial R_c} = \frac{bR_c\sqrt{3(\phi_A + \phi_B)\phi_A\phi_B}}{R_v^3} - \frac{9b\phi_C R_c^2}{4R_v^6\sqrt{3(\phi_A + \phi_B)\phi_A\phi_B}} \times \left[\frac{f_A(R^2 - R_c^2)}{G_2^2}(2\phi_A\phi_B + \phi_B^2) + \frac{f_B R_c^2}{G_1^2}(2\phi_A\phi_B + \phi_A^2)\right]$$

$$\frac{\partial \Delta g_{el}}{\partial (R - R_c)} = \frac{\phi_C}{(r_A + r_B)(R - R_c)}\left(\alpha_A^2 - \frac{1}{\alpha_A}\right) \qquad \frac{\partial \Delta g_{el}}{\partial R_c} = \frac{\phi_C}{(r_A + r_B)R_c}\left(\alpha_B^2 - \frac{1}{\alpha_B}\right)$$

temperature, and the solvent viscosity, respectively. For species which are not hard spheres, eq 14 can only provide an equivalent R_h value.

Experimental Section

1. Sample Preparations. Poly(ethylene oxide)–polystyrene diblock (AB) and triblock (ABA) copolymers were synthesized in Mulhouse, France, by anionic polymerization in THF solution.[21-23] They were purified and then characterized primarily by GPC and ^{1}H NMR. Table III lists the compositions and the molecular weights, as well as molecular weight polydispersities, of the samples investigated.

Two procedures were used to prepare micelle solutions in water. In method 1, weighed samples of block copolymers were added to a known amount of water and heated for ca. 1 h at 65 °C before cooling to room temperature. Samples of low molecular weight or rich in PEO formed clear solutions. In method 2, weighed samples of block copolymer were dissolved in tetrahydrofuran (THF). Water (10 mL) was added to this solution (ca. 2–10 mL), and then the THF was removed under vacuum on a rotary evaporator at 30 °C until no trace (<50 ppm) was detectable by gas chromatographic analysis. While some samples formed clear solutions in this way, other samples became deeply turbid as the THF was removed. In these experiments, distilled deionized (Milli-Q) water and HPLC-grade THF (Caledon) were employed.

The stock solutions used for light scattering measurements all had a concentration of $\sim 5 \times 10^{-4}$ g/mL. The dilution by distilled water was made a few days later. The concentration range of the solutions was from 5×10^{-5} g/mL up to the concentration of the stock solution. Since the critical micelle concentration (cmc) for block copolymers is on the order of 1×10^{-6} g/mL,[24] we took the mass concentration of block copolymer as the micelle concentration in the present data analysis procedure. The aqueous solutions were centrifuged at 12 000 rpm (~17 000g) by using a Sorval RC2-B centrifuge for 2 h to remove foreign materials before being transferred into the light scattering cells. The centrifugation could also be used to distinguish coagulation from formation of stable micelle solutions.

2. Light Scattering Measurements. The laboratory-built light scattering spectrometer, equipped with a 50-mW He–Ne laser operated at $\lambda_0 = 632.8$ nm, was used in the present study. The details of the instrumentation have been described elsewhere.[25] The vertically scattered beam was collected over an angular range of 25–135° for either absolute integrated scattered

Table III
PEO–PS Block Copolymer Samples and Their Properties in Water[a]

sample	M_n(total)	A %, wt %	N_A (PEO)	N_B (PS)	I_P	solubility	M_w	$R_{h,mi}$, nm	$R_{h,agg}$, nm	W_{mi}, %
				Diblock Samples						
R33	112 000	89	2260	118	1.3	▽				
R31	72 000	78	1280	152	1.3	▼				
JLM3	69 700	79	1250	141	1.1	▼				
R32	50 800	77	886	113	1.3	□	9.4×10^7	23	73	54
R30	44 000	67	670	137	1.3	▼				
R23	28 700	61	400	108	1.4	□	4.5×10^7	22	70	87
HA13	24 000	33	180	154	1.1	▼				
R41	23 500	84	450	35	1.2	▽	9.0×10^6	19	74	96
N18	21 600	38	180	129	1.4	▼				
R40	14 100	74	237	36	1.2	□	7.5×10^6	15	36	72
R37	13 800	70	218	40	1.3	□				
JLM5	8 500	80	155	16	1.6	▽	3.0×10^6	10	27	79
				Triblock Samples						
R25	109 000	67	2 × 840	346	1.4	♦				
JLM13	70 000	71	2 × 565	195	1.2	♦				
JLM4	20 000	79	2 × 180	40	1.1	◊	3.6×10^6	12	26	84
R51	19 800	91	2 × 205	17	1.4	◊	4.4×10^6	10	27	73
JLM6	18 000	80	2 × 164	35	1.5	◊	7.4×10^6	11	32	61
R19	13 100	69	2 × 102	39	1.4	○	5.2×10^6	12	57	96
HA10	11 000	73	2 × 91	29	2.7	○				
R46	9 600	60	2 × 66	37	1.4	○				
HA7	7 050	26	2 × 21	50	1.2	♦				

[a] M_n: molecular weight of PEO–PS copolymer molecules determined mainly by GPC. A %: weight percentage of PEO in the sample. N_A and N_B: repeating units of PEO and PS, respectively. Solubility: dissolution tests were performed with copolymer concentrations all being $\sim 5 \times 10^{-4}$ g/mL. ▽ and ◊: solubilized in water at ~60 °C. □ and ○: dissolved in a water–THF mixture (1:1) and a micelle solution forms after THF is removed. ▼ and ♦: soluble in THF; a milky suspension forms and then precipitates once water is added or THF is removed. I_P: index of molecular weight polydispersity. $M_{w,app}$: apparent weight-averaged particle weight of PEO–PS association in water. $R_{h,agg}$ and $R_{h,mi}$: hydrodynamic radii of micellar aggregates and micelles, respectively. W_{mi}, %: weight percentage of micelle in solution.

density or photon correlation spectroscopy measurements. For spherical particles the scaled characteristic line width (Γ/K^2) should be independent of scattering angle if we use the Laplace inversion to obtain the line-width distribution. Thus, only a few angles, typically from 35° to 90°, were measured for the correlation function. The same Γ/K^2 values measured over these angles were obtained within the experimental error limit.

In static light scattering measurements, three to four concentrations for each sample were measured in order to use Zimm plots to obtain the doubly extrapolated (concentration and angle) excess Rayleigh ratio R^0_{vv}. As stated elsewhere,[15] the information obtained from the angular dependence of the excess Rayleigh ratio of an optically inhomogeneous copolymer is related only to an apparent radius of gyration in a complicated weighting form. We have omitted the analysis of the angular and concentration dependence of the excess Rayleigh ratio. In applying eq 10 to calculate the micelle weight M_w, we used a value of $(\partial n/\partial C)_A = 0.134$ at $\lambda_0 = 632.8$ nm[26] and $(\partial n/\partial C)_B = 0.241$ at $\lambda_0 = 589$ nm[27] assuming that the wavelength dependence of $(\partial n/\partial C)_B$ is negligible.

Results and Discussion

1. Phase Diagram. Not all samples we examined formed stable micelles in water. Some, indicated by the open points in Figure 1, formed clear solutions simply by warming mixtures of the polymer and water. Others could be induced to form clear micellar solutions by first dissolving the polymer in THF, diluting with a larger volume of water, and removing all of the THF by distillation under reduced pressure. These samples are indicated by the half-filled points in Figure 1. Many samples could not be induced to form stable micelles under these conditions (filled points, Figure 1). Rather, as the THF evaporated, the solutions turned milky, and the polymer precipitated.

These results allow us to construct the phase diagram shown in Figure 1. It appears that, for high molecular weight samples, micelles form only when the weight fraction of PS is less than 0.25. For lower molecular weight samples the system is more forgiving, and stable micelles containing as much as 40 wt % PS can be formed.

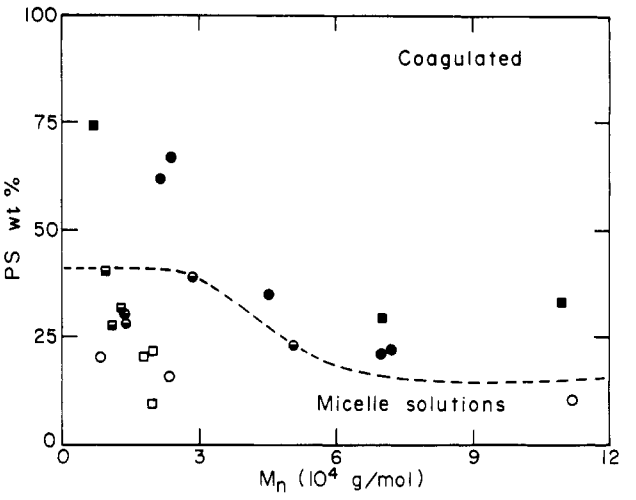

Figure 1. Phase diagram of PEO–PS di- or triblock copolymers in water. Squares: diblock copolymer. Circles: triblock copolymers. Filled symbols: insoluble in water or coagulated once THF was removed from a THF–water mixture. Half-filled symbols: solubilized in THF or THF–water mixtures; a stable micelle solution could form after removal of THF. Hollow symbols: soluble in water.

2. Apparent Micelle Weight and Aggregation Number *N*. The Hilderbrand solubility parameters for polystyrene (=19 $MPa^{1/2}$) and poly(ethylene oxide) (=22.7 $MPa^{1/2}$) are both very close to that of THF (=18.6 $MPa^{1/2}$) but far away from the value for water (=48 $MPa^{1/2}$).[28] The dissolution of PEO–PS block copolymers in water must be mainly driven primarily by forces associated with hydrogen bonding and interactions between EO units and water, leading to local changes in water structure. These interactions not only drive the solubilization of PEO in water but also are responsible for some remarkable properties of PEO in water.[26,29] One interesting but, from

Table IV
PEO-PS Block Copolymer Micelles in Water[a]

sample	M_n (total)	A% (wt%)	$R_{h,mi}/\phi$, nm	$R_{h,agg}/\phi$, nm	N	R_c, nm	S_{EO}, nm^2	V_{EO}, nm^3	L_{mean}, nm	$\chi_{PEO-water}$	χ_{PEO-PS}
Diblock Samples											
R32	50 800	77	0.19	0.58	303	11.0	5.0	0.17	51	0.69	0.030
R23	28 700	61	0.29	0.91	292	10.7	4.9	0.34	23	0.58	0.019
R41	23 500	84	0.28	1.10	119	5.4	3.1	0.52	31	0.55	0.034
R40	14 100	72	0.32	0.76	121	5.5	3.1	0.47	16	0.55	0.022
JLM5	8 500	80	0.31	0.84	63	3.4	2.3	0.41	12	0.57	0.030
Triblock Samples											
JLM4	20 000	79	0.33	0.72	38	3.9	2.5	0.51	13	0.55	0.028
R51	19 800	91	0.29	0.79	19	2.3	1.8	0.53	17	0.55	0.024
JLM6	18 000	80	0.33	0.95	34	3.6	2.4	0.48	12	0.56	0.029
R19	13 100	69	0.46	2.20	38	3.8	2.4	0.90	7.6	0.43	0.001

[a] $\phi \equiv N_A^{3/5}N_B^{4/25}$ for diblock samples and $\phi \equiv N_A^{3/5}N_B^{4/25}2^{-19/25}$ for triblock samples. S_{EO} ($\equiv 4\pi R_c^2/N$ for diblock samples and $4\pi R_c^2/2N$ for triblock samples) is the core surface area per EO block. N: average aggregation number. R_c: micelle core size. V_{EO}: average volume per EO unit in the shell. L_{mean}: shell thickness calculated according to de Gennes' brush model.

our point of view, rather irritating property of PEO in water is its tendency to undergo reversible self-association.[26,30,31,32] In the present system of PEO-PS block copolymers in water, the core-corona micelles have long PEO chains in the outer layer in contact with water. Some secondary association or aggregation between PEO chains occurs to form micelle clusters which coexist with the regular micelles. This phenomenon greatly confuses the molecular weight measurement by SLS, particularly since the extent of micelle aggregation, while small, varies from sample to sample. Because the secondary aggregates have a much larger mass than that of micelles, only a very small amount of aggregates causes a strong scattering intensity to be superimposed on the scattered intensity produced by the micelles themselves. For example, reports in the literature indicate that the sample R41 has been characterized by SLS in three different laboratories[23,33] at different times. Values for the apparent micelle weight were all different: $M_{w,app} = 2.4 \times 10^6$ in ref 33, $M_{w,app} = 3.6 \times 10^7$ in ref 23, and $M_{w,app} = 9.0 \times 10^6$ in the present study. To get a correct micelle weight, the measured R_{vv}^0 values have to be decomposed to obtain separately the scattering intensity contributed by the micelles and by the micellar aggregates.

Because species of different sizes have different translational diffusion coefficients, they yield different characteristic line widths in a QELS measurement. This information is contained in the line-width distribution function $G(\Gamma)$ as described in eq 11. Recently, advances in data analysis make it possible to carry out a Laplace inversion of $G(\Gamma)$ from photon correlation spectroscopy to obtain the distribution of diffusing species without previous (or preset) knowledge about its form.[34] In bimodal distributions, the two peaks and their relative populations (and their hydrodynamic radii for spherical particles) can be determined if their line-width ratio is ≥ 2.[35] Due to the nature of the ill-posed Laplace inversion and imperfections in the measured data, the distribution shape, the weight percentages of the two peaks, and the hydrodynamic radii resolved from Laplace inversion have an uncertainty ranging from 5% to 15%.[36] In the present study, we found bimodal distributions present in all of the samples investigated. The ratios of the two line widths of each sample, Γ_1/Γ_2, were always larger than 2, mostly larger than 2.5, well within our resolution limit. In an earlier publication, we showed a typical line-width distribution for a PS-PEO micelle solution in water, resolved by Laplace inversion from photon correlation spectroscopy in QELS measurements.[15] Here we report that, by repeating the measurements at the same or different scattering vectors and at various polymer concentrations,

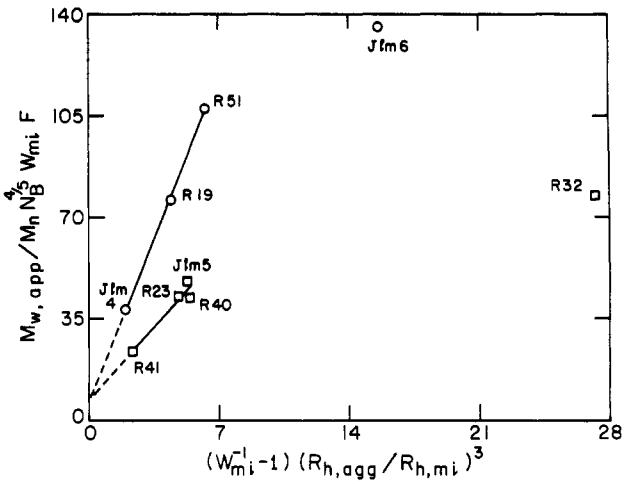

Figure 2. Plot for decomposition of the apparent particle weight to resolve the proportionality constant A. Squares: diblock copolymers, $M_{w,app}/(M_n N_B^{4/5} W_{mi} F) = 6.89 + 7.23(W_{mi}^{-1}-1)(R_{h,agg}/R_{h,mi})^3$. Circles: triblock copolymers, $M_{w,app}/(M_n N_B^{4/5} W_{mi} F) = 6.84 + 15.9(W_{mi}^{-1}-1)(R_{h,agg}/R_{h,mi})^3$.

the uncertainty involved in determining W_{mi}, the weight percentage of the micelle population, is ~15% and that of R_h is ~7%. Table III lists the LS results for the nine samples investigated where the values of W_{mi} are averages over several measurements.

2.1. Test of the Star Model. One of the key predictions of the star model, eqs 5 and 8, is that $R \propto FN_B^{4/25}N_A^{3/5}$. To test this prediction, we choose R_h as the characteristic radius and calculate the ratio $R/FN_B^{4/25}N_A^{3/5}$ for each of the samples which form micelles. In Table IV we see that this ratio is constant for seven of our nine samples of block copolymer micelles but that it is not constant for the larger secondary aggregates. We take the constancy of this ratio as providing strong evidence for the validity of the star model.

2.2. Obtaining Aggregation Numbers. Zimm plots of our SLS data provide apparent molecular weights $M_{w,app}$ which represent a weighted average of the two species, micelles and secondary aggregates, present in solution. To proceed, we now *assume* the validity of the star model and introduce the prediction that $N \propto N_B^{4/5}$ into our data analysis. According to the definition of the weight-averaged molecular weight

$$M_{w,app} = W_{mi}M_{mi} + (1 - W_{mi})M_{agg} = AFW_{mi}M_nN_B^{4/5} + BF(1 - W_{mi})M_nN_B^{4/5}(R_{h,agg}/R_{h,mi})^3 \quad (15)$$

which can be rearranged into

$$\frac{M_{w,app}}{FW_{mi}M_nN_B^{4/5}} = A + B\left(\frac{1}{W_{mi}} - 1\right)\left(\frac{R_{h,agg}}{R_{h,mi}}\right)^3 \quad (16)$$

In eqs 15 and 16 A and B are two proportionality constants; F is the correction factor for applying the star model to triblock samples; i.e., $F = 1$ for diblock samples and $F = 2^{-9/5}$ for triblock samples. It should be noted that in the above formulation we have neglected the polydispersity and their differences between samples. The effects of compositional and mass polydispersity on the data analysis have been merged into the proportionality constants A and B and may be responsible for some of the scatter in our plots. The bias caused by sample polydispersity will be partially compensated in the global fitting of A and B from various samples, and hopefully errors associated with these assumptions are not significant.

Since eq 16 is linear, the proportionality constants A and B can be fitted from a graphical analysis of measured values of $R_{h,agg}$, $R_{h,mi}$, $M_{w,app}$, and W_{mi}. Figure 2 shows such a plot. Aside from samples Jlm6 and R32, data from triblock and diblock samples, respectively, fall on two straight lines which have different slopes (B) but a common intercept (A). This result implies that both triblock and diblock copolymer micelles have a similar star-shaped structure, and the assumption of each triblock molecule being considered as two diblock molecules is a good approximation. The different B values indicate that aggregates of triblock copolymer micelles and of diblock micelles have a different macrostructure; i.e., triblock copolymer micelle secondary aggregates have a denser packing. Taking $A = 6.9$, the mean aggregation number N for the various micelles can be calculated. These values are presented in Table IV. They indicate that the aggregation number increases either as the molecular weight increases or as the PS content in the copolymer increases. Diblock copolymer micelles have a higher aggregation number than those of triblock copolymer micelles.

Because of the high hydrophobicity of PS, we assume that the core is water-free. We can than compute the core radius R_c, the core surface area per EO block S_{EO}, and the average volume occupied by per EO unit in the shell V_{EO}. These values are listed in Table IV.

It is important to recognize that the polymers we examine have a relatively limited range of N_B values, from 16 to 108 for diblock copolymers and from 17 to 40 for triblock copolymers. Recasting eq 15 in terms of the mean-field model prediction that $N \propto N_B$ introduces only a very small difference in the data analysis.

3. Concentration Profile of EO Segments in the Corona. One of the key differences between the mean density models and the star model is that the latter specifically takes account of the decrease in ϕ_A with increasing radial distance from the core. The mean density model neglects this decrease but allows for the possibility that different micelles with different N_A and N_B values will have different mean $\langle\phi_A\rangle$ values in the corona. We now take this approach and calculate $\langle\phi_{PEO}\rangle$ values for each of our samples.

In particular, we focus on the water content of the corona. The term V_{EO} contains three contributions, the volume of the EO segment itself (0.0646 nm^3),[10] the volume of the two water molecules (0.030 nm^3 each) directly hydrogen-bonded to each EO unit,[10] and the water which occupies the remaining space inside the swollen coils. The hypothetical minimum corona volume would contain only two water molecules per EO and $V_{EO,min} = 0.125$ nm^3.

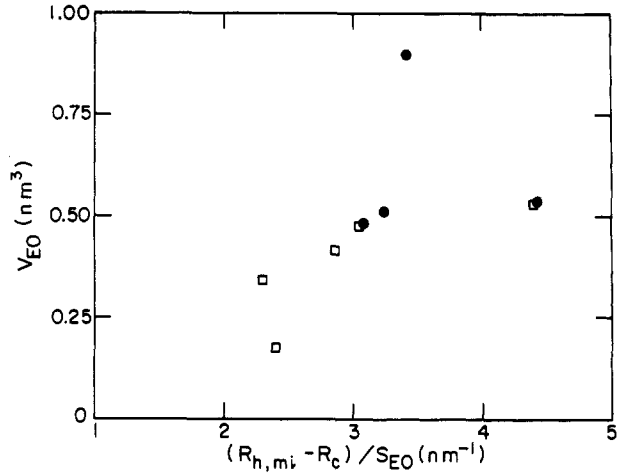

Figure 3. $(R_{h,mi} - R_c)/S_{EO}$, which is the shell thickness of micelles scaled by the core surface area per EO block, versus the volume occupied by per EO unit V_{EO}. Squares: diblock copolymer micelles. Filled circles: triblock copolymer micelles.

To examine the sample-to-sample variation in V_{EO}, we plot this value in Figure 3 against the corona thickness ($L = R_{h,mi} - R_c$) divided by the surface area per polymer chain S_{EO}. V_{EO} is a mean value, a measure of $\langle\phi_{PEO}\rangle$. Nevertheless, the plot in Figure 3 indicates that the volume occupied per EO segment increases with increasing shell thickness. Interestingly, extrapolating this plot to a thin finite shell with $L/S_{EO} = 1$ gives a value of V_{EO} close to the minimum value of 0.13 nm^3.

The micelle mean density model in many ways resembles the brush model[6,7] developed to describe long soluble chains end-grafted onto a flat nonadsorbing surface. For such a system the layer thickness L can be calculated as $L = N_A\mathbf{a}\sigma^{1/3}$ provided that the density (σ) of grafted sites is high enough ($N_A^{1.2}\sigma > 1$) that the mean spacing between chains is smaller than the radius of gyration of an A coil in good solvent. Here $\mathbf{a}$ is the mesh diameter of the lattice.

It is instructive to compare our experimental values of L obtained with values L' calculated by the brush model for adsorption on a flat surface. In the spherical micelle case, the surface area is $4\pi R_c^2$. If we take $\mathbf{a}$ to be 0.25 nm for an EO unit,[15] the condition $N_A^{1.2}\sigma = (\mathbf{a}^2 N N_A^{1.2})/(4\pi R_c^2) > 1$ is fulfilled in our samples. We calculate L' from the expressions

$$L' = N_A\mathbf{a}\left(\frac{N\mathbf{a}^2}{4\pi R_c^2}\right)^{1/3} \text{ (diblock copolymer)} \quad (17a)$$

$$L' = \frac{N_A\mathbf{a}}{2}\left(\frac{N\mathbf{a}^2}{2\pi R_c^2}\right)^{1/3} \text{ (triblock copolymer)} \quad (17b)$$

The L' values are consistently larger even than the R_h values for the micelles as listed in Table IV. A log–log plot of L' vs $(R_h - R_c)$ is fitted by a straight line with a slope of 1.33 (Figure 4). In the brush geometry, especially at distances far from the surface, the A chains are squeezed into a smaller space and become much more elongated than those attached to a spherical surface, yielding an increasing of corona thickness.

4. χ Parameters. PEO–Water. Given the number of assumptions made in analyzing our data, we initially took a very skeptical attitude toward any χ values that we might obtain by inserting values of N, R_c, and R_h (=R) into eqs 8 and 9. Indeed, a glance at the $\chi_{PEO-water}$ column of Table IV shows that these values range from 0.69 to 0.43, and a surface polymer with a χ_{AS} value greater than 0.5 would

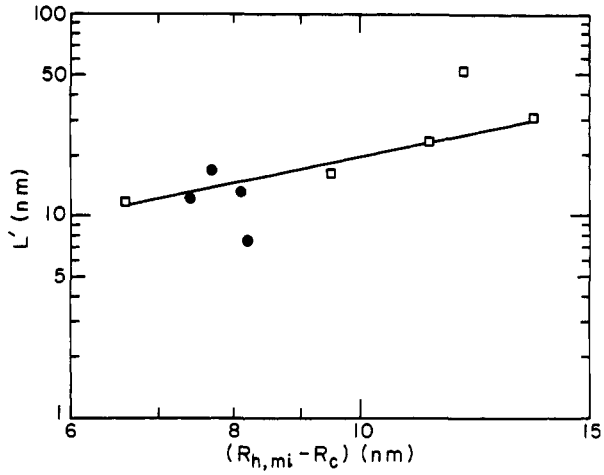

Figure 4. Plot of micelle shell thickness deduced from the star model versus that from the mean density model prediction. Squares: diblock copolymer micelles. Filled circles: triblock copolymer micelles.

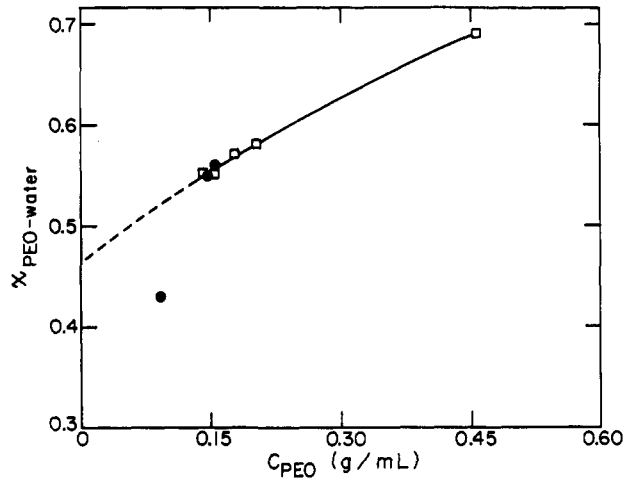

Figure 5. Plot of $\chi_{PEO-water}$ versus the average PEO concentration in the shell. Squares: diblock copolymer micelles. Filled circles: triblock copolymer micelles.

not be a very effective steric stabilizer. Our attitude changed once we realized that values for $\chi_{PEO-water}$ are concentration dependent.[37,38] For example, for linear PEG of M_w = 5000 in water at 65 °C, Malcolm et al.[37] found that $\chi_{PEO-water}$ values were 0.4, 0.75, and 1.24 when the volume fraction of PEG increased from 0.25 to 0.66 and to 0.9, respectively. To our great surprise, when the $\chi_{PEO-water}$ values listed in Table IV were plotted against $\langle\phi_{PEO}\rangle$ of different samples, all but one of the data points fell on a single curve. This result is shown in Figure 5, where the x axis (C_{PEO}) is the mean concentration (g/mL) of PEO in the corona.

Our results not only are consistent with independent determinations of $\chi_{PEO-water}$—the extrapolation in Figure 5 yields $\chi_{PEO-water,c\to 0}$ = 0.47 while $\chi_{PEO-water}$ in very dilute solution is close to 0.4–0.45[39,40]—but they also tell us something quite significant about the steric stabilizing behavior of PEO chains. PEO provides effective micellar stabilization only because, at the fringes of the micelle, the local concentration of PEO is sufficiently small that the coils resist interpenetration. This result also provides an explanation for the transient stability of the secondary aggregates of micelles. Once interpenetration of PEO chains occurs, the local concentration can be high enough that the PEO interactions are attractive.

We attempt, in Figure 6, to estimate the χ parameter profile in our micelles as a function of the radial distance

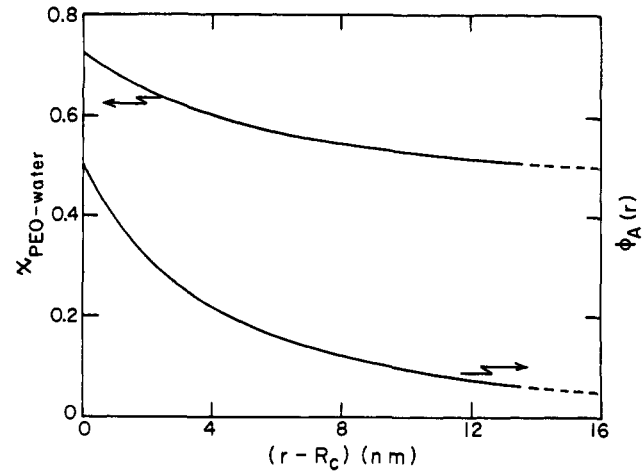

Figure 6. Profiles of monomer volume fraction of EO and $\chi_{PEO-water}$ in the micelle shell as functions of distance from the core surface assuming that $\phi_A(R_c)$ = 0.5 for sample R41.

from the core. In the star model the monomer volume fraction in the shell decreases as $r^{-4/3}$:

$$\phi_A(r) = A_\phi N^{3/2} r^{-4/3} + B_\phi \tag{18}$$

where r is the distance from the center of micelle and A_ϕ and B_ϕ are two proportionality constants. One needs two boundary conditions to deduce A_ϕ and B_ϕ. One condition is the average volume fraction of PEO in the shell

$$\langle\phi_A\rangle = \frac{3\int_{R_c}^{R} r^2\phi_A(r)\,dr}{R^3 - R_c^3} = \frac{3NN_A\nu_{EO}}{4\pi(R^3 - R_c^3)} \tag{19}$$

with ν_{EO} (=0.0646 nm^3) being the monomer volume per EO unit. The second boundary condition depends upon the volume fraction of EO at the interface between the core and the shell, $\phi_A(R_c)$. Since EO chains may fold back to the core surface, $\phi_A(R_c)$ will be considerably larger than σ. We found that there is a range of $\phi_A(R_c)$ values where the solution for A_ϕ and B_ϕ, and consequently $\phi_A(R)$, still is meaningful. For example, for sample R41, the range is $0.15 < \phi_A(R_c) < 0.85$. If we take $\phi_A(R_c)$ = 0.5, we can obtain a concentration profile of EO in the shell after solving eq 18 for A_ϕ and B_ϕ. Figure 6 shows $\phi_A(r)$ for sample R41 as a function of the distance from the core surface, as well as the $\chi_{PEO-water}$ profile in the shell. We notice that the $\chi_{PEO-water}$ value is reduced to less than 0.5 only in a region very close to the surface of the micelle.

PS–PEO. The values obtained for χ_{PEO-PS} in the present study show good sample-to-sample reproducibility and, except for R19, do not vary significantly with polymer composition or microstructure. The values all fall in the range of 0.02–0.03 and are in good agreement with values obtained by Nagata et al.[41] in their light scattering studies of PEO in PS–bromobenzene mixtures under "optical Θ-conditions". These authors point out that χ_{AB} values in dilute solution differ from those in bulk because of the influence of excluded-volume effects in solution, which decreases the number of AB contacts. When they correct for excluded-volume effects, their dilute-solution value of χ_{PEO-PS} = 0.02 yields a value of χ_{PEO-PS} = 0.28, which they believe is more representative of the value in the bulk state.

There is a lot of current interest in this value, and a number of pertinent experiments have been reported by several scientists at Xerox, both in Mississauga, Ontario, and in Webster, NY. DiPaola-Baranyi[42] has used inverse gas chromatography to study PS–PEO block copolymers

in the melt at 150 °C. She calculates $\chi_{PEO-PS} = 0.3$ from the data at that temperature. Smith and co-workers[43] have examined the micelles formed when PS–PEO diblocks rich in PS are mixed with a PS matrix, also at 150 °C. Their data are consistent with the Whitmore–Noolandi model[44] if they use values χ_{PEO-PS} close to 0.3. Taken together, these studies all point to a χ_{PEO-PS} value close to 0.3 over a wide temperature range.

On the other hand, Chow has examined the influence of PS on the melting point of PEO for PS–PEO diblock copolymer films prepared by solvent casting and from the melt. His model allows him to calculate χ parameters from melting point depression data and yields values of χ_{PEO-PS} that vary with composition, but which all fall in the range of −0.2 to −0.3.[45] This value is very much at odds with the values reported above. A negative χ_{PEO-PS} value at 150 °C would be inconsistent with the formation of PS–PEO micelles in a PS matrix. It appears that there are ambiguities among these various experiments that need to be resolved.

Summary

PS–PEO diblock and PEO–PS–PEO triblock copolymers form spherical micelles in water for samples not too rich in PS. The analysis of the micelle in terms of current theory is complicated by the tendency of the micelles to undergo a very small extent of secondary association to form clusters containing 20–30 micelles. These species can be detected, and their respective R_h values determined, by a Laplace inversion analysis of the QELS signal. The R_h values for the micelles are in good accord with the scaling relationship of Halperin's star model.[13]

To proceed further, we incorporate the star model into our data analysis to obtain aggregation numbers N and core radii R_c. With these parameters we are able to test the validity of the Noolandi–Hong mean density micelle model by using their equations to calculate χ parameters for the interactions of PEO–water and PEO–PS. The values we obtain are in very good agreement with values in the literature, and our most definitive result is the linear dependence of $\chi_{PEO-water}$ on PEO concentration. Our results thus provide very good support for two very different models of block copolymer micelle formation in solution.

Acknowledgment. We thank the NSERC of Canada and the Province of Ontario for their support of this research. We thank Dr. J. Noolandi for helpful discussions on the mean density model. We thank Dr. G. DiPaola-Baranyi at the Xerox Research Centre of Canada and Dr. T. Smith at the Xerox Webster Research Centre for permission to cite their as yet unpublished data. B.C. acknowledges support of his work by the NSF (Grant DMR 8921968).

References and Notes

(1) The series on polymer micelle formation are as follows: No. 1: Zhao, C.; Winnik, M. A. *Langmuir* **1990**, *6*, 514. No. 2: ref 15 of this article. No. 3: ref 24 of this article. No. 4: Xu, R.; Hu, Y.; Winnik, M. A.; Riess, G.; Croucher, M. *J. Chromatogr.* **1991**, *547*, 434. No. 6: Xu, R.; d'Oliveria, J.; Winnik, M. A.; Riess, G.; Croucher, M. D. *J. Appl. Polym.*, in press.
(2) A recipient of a Postdoctoral Fellowship awarded by the NSERC of Canada. Present address: Coulter Corp., 600 West 20th Street, Hialeah, FL 33010.
(3) Tuzar, Z.; Kratochvil, P. *Colloids Surf.*, in press.
(4) Tuzar, Z.; Kratochvil, P. *Adv. Colloid Interface Sci.* **1976**, *6*, 201.
(5) Riess, G.; Hurtrez, G.; Bahadur, P. In *Encyclopedia of Polymer Sciences and Engineering*, 2nd ed.; Mark, H., Bikales, N. M., Overberger, C. G., Menges, G., Eds.; John Wiley & Sons: New York, 1985; Vol. 2, pp 324–436.
(6) Alexander, S. *J. Phys. (Paris)* **1977**, *38*, 977, 983.
(7) de Gennes, P.-G. In *Solid State Physics*; Liebert, J., Ed.; Academic: New York, 1978; supplement 14, p 1.
(8) Noolandi, J.; Hong, M. H. *Macromolecules* **1983**, *16*, 1443.
(9) Leibler, L.; Orland, H.; Wheeler, J. C. *J. Chem. Phys.* **1983**, *79*, 3550.
(10) Nagarajan, R.; Ganesh, K. *J. Chem. Phys.* **1989**, *90*, 5843.
(11) Munch, M. R.; Gast, A. P. *Macromolecules* **1988**, *21*, 1360.
(12) Vagberg, L. J. M.; Cogan, K. A.; Gast, A. P. *Macromolecules*, preprint.
(13) Halperin, A. *Macromolecules* **1987**, *20*, 2943.
(14) Cogan, K. A.; Gast, A. P. *Macromolecules* **1990**, *23*, 745.
(15) Xu, R.; Winnik, M. A.; Hallett, F. R.; Riess, G.; Croucher, M. D. *Macromolecules* **1991**, *24*, 87.
(16) Tucker et al. report that the T_g of the PS phase of PS diblock copolymers in bulk is lower, for chain lengths corresponding to our samples, than that of a PS homopolymer of similar length. The additional effect of the aqueous environment on the micellar T_g is not known. Tucker, P. S.; Barlow, J. W.; Paul, D. R. *Macromolecules* **1988**, *21*, 2794.
(17) Tanford, C.; Nozaki, Y.; Rohde, M. F. *J. Phys. Chem.* **1977**, *81*, 1555.
(18) Daoud, M.; Cotton, J. P. *J. Phys. (Les. Ulis. Fr.)* **1982**, *43*, 531.
(19) The expressions and the definitions in Table I are taken directly from ref 8. In ref 8, on the right-hand side of eqs 2–10 and 2–11, a term b $(=(b_A + b_B)/2)$ is missing.
(20) Benoit, H.; Froelich, D. In *Light Scattering from Polymer Solution*; Huglin, M., Ed.; Academic Press: London, 1972; Chapter 11.
(21) Riess, G.; Nervo, J.; Rogez, D. *Polym. Eng. Sci.* **1977**, *17*, 634.
(22) Mura, J. L. Doctoral Thesis, University of Haute Alsace, Mulhouse, France, 1991.
(23) Riess, G.; Rogez, D. *Polym. Prepr. (Am. Chem. Soc., Div. Polym. Chem.)* **1982**, *23*, 19.
(24) Wilhelm, M.; Zhao, C.; Wang, Y.; Xu, R.; Winnik, M. A.; Mura, J.; Riess, G.; Croucher, M. D. *Macromolecules* **1991**, *24*, 1033.
(25) Zhou, Z.; Chu, B. *J. Colloid Interface Sci.* **1988**, *126*, 171.
(26) Polik, W. F.; Burchard, W. *Macromolecules* **1983**, *16*, 978.
(27) Alfrey, T., Jr.; Bradford, E. B.; Vanderhoff, J. W. *J. Opt. Soc. Am.* **1964**, *44*, 603.
(28) Barton, A. F. M. *Handbook of Solubility Parameters and Other Cohesion Parameters*; CRC Press: Boca Raton, FL, 1988.
(29) Rowlinson, J. S. *Liquid and Liquid Mixtures*, 2nd ed.; Butterworths: London, 1969; p 167.
(30) Brown, W. *Polymer* **1985**, *26*, 1647.
(31) Devanand, K.; Selser, J. C. *Nature* **1990**, *343*, 739.
(32) In ref 31, the authors claimed that they did not observe PEO aggregation by QELS in carefully prepared PEO aqueous solutions. One should note that the measured average line width $(\bar{\Gamma})$ from QELS is much less sensitive than the integrated scattered intensity to a small amount of large particles especially if the correlation functions were not analyzed by a Laplace inversion method.
(33) Bahadur, P.; Sastry, N. V.; Rao, Y. K.; Riess, G. *Colloids Surf.* **1988**, *29*, 343.
(34) Chu, B.; Ford, J.; Dhadwal, H. In *Methods of Enzymology*; Colowick, S. P., Kaplan, N. O., Eds.; Academic Press: Orlando, FL, 1985; Vol. 117, p 256.
(35) Chu, B.; Xu, R.; Nyeo, S. L. *Part. Part. Syst. Charact.* **1989**, *6*, 34.
(36) Bott, S. E. In *Particle Size Distribution, Assessment and Characterization*; Provder, T., Ed.; ACS Symposium Series 332; American Chemical Society: Washington, DC, 1987; p 74.
(37) Malcolm, G. N.; Rowlinson, J. S. *Trans. Faraday Soc.* **1957**, *53*, 921.
(38) Gnanou, Y.; Hild, G.; Rempp, P. *Macromolecules* **1987**, *20*, 1662.
(39) Strazielle, C. *Makromol. Chem.* **1958**, *119*, 50.
(40) Good, W. R.; Cantow, H.-J. *Polym. Bull.* **1978**, *1*, 115.
(41) Nagata, M.; Fukuda, T.; Inagaki, H. *Macromolecules* **1987**, *20*, 2173.
(42) DiPaola-Baranyi, G., personal communication.
(43) Smith, T.; et al., personal communication.
(44) Whitmore, D.; Noolandi, J. *Macromolecules* **1985**, *18*, 657.
(45) Chow, T. S. *Macromolecules* **1990**, *23*, 333.

Registry No. PS–PEO (block copolymer), 107311-90-0.